

Attribution-NonCommercial 4.0 International (CC BY-NC 4.0)

<https://creativecommons.org/licenses/by-nc/4.0/>

Access to this work was provided by the University of Maryland, Baltimore County (UMBC) ScholarWorks@UMBC digital repository on the Maryland Shared Open Access (MD-SOAR) platform.

Please provide feedback

Please support the ScholarWorks@UMBC repository by emailing scholarworks-group@umbc.edu and telling us what having access to this work means to you and why it's important to you. Thank you.



Asymmetry of leaf internal structure affects PLSR modelling of anatomical traits using VIS-NIR leaf level spectra

Eva Neuwirthová, Zuzana Lhotáková, Lucie Červená, Petr Lukeš, Petya Campbell & Jana Albrechtová

To cite this article: Eva Neuwirthová, Zuzana Lhotáková, Lucie Červená, Petr Lukeš, Petya Campbell & Jana Albrechtová (2024) Asymmetry of leaf internal structure affects PLSR modelling of anatomical traits using VIS-NIR leaf level spectra, European Journal of Remote Sensing, 57:1, 2292154, DOI: [10.1080/22797254.2023.2292154](https://doi.org/10.1080/22797254.2023.2292154)

To link to this article: <https://doi.org/10.1080/22797254.2023.2292154>



© 2023 The Author(s). Published by Informa UK Limited, trading as Taylor & Francis Group.



Published online: 18 Dec 2023.



Submit your article to this journal [↗](#)



Article views: 428



View related articles [↗](#)



View Crossmark data [↗](#)

Asymmetry of leaf internal structure affects PLSR modelling of anatomical traits using VIS-NIR leaf level spectra

Eva Neuwirthová ^a, Zuzana Lhotáková ^a, Lucie Červená ^b, Petr Lukeš ^c, Petya Campbell ^d
and Jana Albrechtová ^a

^aDepartment of Experimental Plant Biology, Faculty of Science, Charles University, Prague, Czech Republic; ^bDepartment of Applied Geoinformatics and Cartography, Faculty of Science, Charles University, Prague, Czech Republic; ^cGlobal Change Research Institute, Czech Academy of Sciences, Brno, Czech Republic; ^dNASA Goddard Space Flight Center; Goddard Earth Sciences Technology and Research (GESTAR) II, University of Maryland Baltimore County, Greenbelt, MD, USA

ABSTRACT

Leaf traits can be used to elucidate vegetation functional responses to global climate change. Pigments, water and leaf mass per area are the most used traits. However, detailed anatomical traits such as leaf thickness, the thickness of palisade and spongy parenchyma are often neglected, although they affect leaf physiological function and optical properties. Our aim was to produce partial least squares regression (PLSR) models for estimating leaf traits using biconical reflectance factor (BCRF). We established that estimation of leaf anatomical properties differs when using BCRF obtained from the upper and lower surface of the leaf. PLSR explained that 90% of the variability was based on total chlorophyll content ($R^2 = 0.95$), spongy parenchyma to leaf thickness ratio ($R^2 = 0.94$), equivalent water thickness ($R^2 = 0.93$) and leaf mass per area ($R^2 = 0.91$) or leaf thickness ($R^2 = 0.90$). We conclude that internal asymmetry in leaf structure affects significantly leaf optical properties and should not be neglected in radiative transfer modelling at the leaf level and when upscaling leaf properties to the canopy.

ARTICLE HISTORY

Received 10 November 2022
Revised 8 September 2023
Accepted 4 December 2023

KEYWORDS

Planar leaves; leaf thickness; palisade; spongy parenchyma; contact probe; two-sided reflectance; leaf optical properties; leaf traits; vegetation function




Introduction

Global climate change directly affects ecosystem properties through changes in plant functional traits and metabolism of the organisms, which in turn affect a range of ecosystem functions and services (Díaz et al., 2007). Due to mutual relation, plant functional traits can be used to predict the response of ecosystem function, which is mainly driven by photosynthesis (He et al., 2018; Liu et al., 2019). Maximum photosynthetic rate (McClendon, 1962) and photosynthetic efficiency (Kenzo et al., 2004) are influenced by leaf structural traits and are closely related to gross primary productivity (He et al., 2018). In a study by Niinemets (2001), relationships between leaf structure and long-term climatic variables were observed, and later (He et al., 2018) demonstrated that leaf anatomy and internal structure are significantly correlated with annual temperature and precipitation.

The anatomy and biochemistry of a leaf depends on the local environmental conditions in which the plant develops and the leaf grows. Higher temperature and incident solar radiation result in higher leaf thickness (LT) (Niinemets, 2001) and higher leaf mass per area (LMA) (Yang et al., 2014), which usually show higher leaf tolerance to drought and irradiance stress (Hallik

et al., 2019). As a result of the irradiance gradient, LT, leaf mass per area and palisade parenchyma (PP) thickness increase with canopy height (Zhang et al., 2019). LT is positively related to leaf mass per area and also to leaf mass density (LD) (Villar et al., 2013). Increasing of the LT and leaf mass per area during the leaf development is due to the expansion of PP cells and accumulation of photosynthetic pigment (Neuwirthová et al., 2021). Also, the ratio of PP thickness to spongy parenchyma (SP) thickness is driven by the leaf development and it increases during the season (Lukeš et al., 2020). Thicker leaves have thicker PP and higher leaf mass per area (Zhang et al., 2019) and also tend to have a higher photosynthetic pigment content (Cao, 2000).

Chlorophyll content is not a single indicator of the photosynthetic rate, the leaf porosity (proportion of intercellular spaces) and mass density must also be considered. A higher number of PP cells, with a higher leaf mass density, results in reduction of photosynthetic rate due to lower CO₂ conductance (Niinemets, 2001). The amount of internal leaf surface area available for CO₂ diffusion, usually expressed as the area of mesophyll cells exposed to intercellular spaces per unit leaf area, is critical for mesophyll

CONTACT Eva Neuwirthová  eva.neuwirthova@natur.cuni.cz; Jana Albrechtová  jana.albrechtova@natur.cuni.cz  Department of Experimental Plant Biology, Faculty of Science, Charles University, Viničná 5, Prague 212844, Czech Republic

© 2023 The Author(s). Published by Informa UK Limited, trading as Taylor & Francis Group.

This is an Open Access article distributed under the terms of the Creative Commons Attribution-NonCommercial License (<http://creativecommons.org/licenses/by-nc/4.0/>), which permits unrestricted non-commercial use, distribution, and reproduction in any medium, provided the original work is properly cited. The terms on which this article has been published allow the posting of the Accepted Manuscript in a repository by the author(s) or with their consent.

CO₂ conductance, and thus for CO₂ assimilation (Hanba et al., 1999; Slaton & Smith, 2002).

Using leaf optical properties, it is possible to estimate not only the content of photosynthetic pigments in the leaf (Gates et al., 1965) but also the leaf anatomical structure (Buschmann et al., 2012; Neuwirthová et al., 2021; Shull, 1929; Slaton et al., 2001). It is generally accepted that the reflectance in the near infrared region (NIR; 750–1350 nm) (Eitel et al., 2006; Gates et al., 1965) is influenced by the LT (Knapp & Carter, 1998) and leaf internal structure (ratio of mesophyll cell surface area per unit leaf surface area (Slaton et al., 2001)). In a previous study, we estimated structural parameters acting as leaf functional traits, such as specific leaf area, LT and SP ratio, which can be retrieved from leaf optical properties (Neuwirthová et al., 2021).

Leaf optical properties are known to differ from upper and lower leaf side (Buschmann et al., 2012; Lukeš et al., 2020). In 1971, Woolley described that a higher fraction of airspaces results in increased ratio of reflectance to transmittance at all wavelengths in the 400–2500 nm region. Long PP cells, which have an anisotropic arrangement, may facilitate light penetration deeper into the leaf interior, whereas multilobbed spongy mesophyll cells with a more isotropic structure tend to scatter radiation (Borsuk et al., 2022; Vogelmann, 1993).

The importance of considering leaf asymmetry (i.e. the variation in the data and the error due to not considering the asymmetry) differs for different species and species groups. For example, it is more important for plants which change their leaf orientation a lot due to changes in environmental conditions (i.e. heliotropic plants) because the reflectance spectra will be affected by the lower and upper leaf side signals at different proportions. For example, in response to high PAR, common bean (*Phaseolus vulgaris* L., (Pastenes, 2004)) and some leguminous tree species (e.g. *Prosopis tamarugo* Phil., (Chávez et al., 2014)) orient their leaves with the adaxial surface away from the sun. Other tree species (e.g. *Populus tremuloides* Michx) flutter their leaves in the wind due to flattened and flexible petiole, which also results in temporal exposition of the leaf abaxial side upwards (Niklas, 1991; Roden, 2003). Due to water deficiency, maize (*Zea mays* L.) curls/rolls its leaves up and a sensor will see primarily the lower side, which results in changes in leaf reflectance and also in fluorescence emissions, which are indicative of plant stress (Campbell et al., 2007, 2019). When estimating canopy reflectance, the error associated with ignoring the differences in upper and lower leaf side optical properties is likely higher for deciduous vs. coniferous canopies, since conifers have lower ability to re-orient their foliage in response to the short-term environmental variations (Middleton et al., 2018).

In our previous study (Lukeš et al., 2020), we used this assumption to simulate the optical properties of leaves from both the upper (adaxial) and lower (abaxial) sides in a leaf-level radiative transfer model called the Dorsiventral Leaf Model (DLM) (Stuckens et al., 2009). The dorsiventral leaf reflectance simulated this way were upscaled to the canopy level (top of canopy, TOC reflectance) by coupling the simulation results of the leaf-level DLM model with a whole canopy model called Discrete Anisotropic Radiative Transfer model (DART) (Gastellu-Etchegorry et al., 2004). We were thus able to quantify the effect of a simplified parameterization of optical properties in which dorsiventral asymmetry is typically neglected on the TOC reflectance. The main conclusions of the previous study (Lukeš et al., 2020) were that the neglecting differences in lower (abaxial) side leaf reflectance may introduce relative difference up to 20%, causing the underestimation of “one-sided” scenario compared to “two-sided” one.

The aim of the present study was to construct partial least squares regression (PLSR) models to predict leaf biophysical traits from leaf biconical reflectance factor (BCRF) measured from both upper (adaxial) and lower (abaxial) leaf sides. We hypothesized that the estimation of leaf anatomical properties would differ, if either BCRF obtained from the upper (commonly used in RS), or BCRF from both the adaxial and abaxial sides of the leaves served as input to the PLSR model.

Material and methods

Leaves were collected from trees growing either in the outdoor exhibitions or from inside collection at the Botanical Garden of Charles University in Prague (50.072N, 14.424E). Plants were selected considering their internal leaf structure representing leaves of woody plants with a typical dorsiventral leaf structure (composed of an upper epidermis, photosynthetic tissue differentiated into palisade and spongy mesophyll and lower epidermis). We included typical mesomorphic leaves of temperate broadleaved tree species and woody species representatives with xeromorphic leaf structure, which for the analysis in this study were organised in three groups. Group one includes typical dorsiventral leaves of common temperate deciduous tree species (temperate broadleaved = TB) (*Acer campestre* L., *Acer platanoides* L., *Carpinus betulus* L., *Corylus maxima* Mill., *Quercus robur* L. and *Tilia euchlora* C. Koch). All species in this group were sampled in outdoor exhibitions. Group two includes xeromorphic, thick leaves of *Ficus* sp. with pronounced epidermis and high PP/SP ratio, i. e. less dense photosynthetic tissue (*Ficus* xeromorphic broadleaf = FXB) (*Ficus benjamina* L., *Ficus lyrata* Warb. and *Ficus triangularis* L.). All sampled species

were grown indoor, excluding seasonal variability typical for temperate region. Group three is comprised of xeromorphic, thick leaves of *Rhododendron* sp. L. (*Rhododendron* xeromorphic broadleaved= RXB) grown outdoor: with pronounced epidermis and low PP/SP ratio, i. e. more dense photosynthetic tissue. Usually, leaves were sampled from the ground, thus effect of the sun or shaded leaves was neglected, and leaves exhibited more shaded structure. Leaf sampling was accomplished three times within the growing season: 29th April; 16th September; 21st October. One to three leaves per plant was sampled.

Leaf reflectance measurements

Leaf spectral reflectance was measured immediately after leaf excision. Leaves were placed on non-reflective background with albedo around 1%. The BCRF at the leaf level was measured by a spectroradiometer ASD FieldSpec 4 Wide-Res with a contact probe (ASD Inc., Boulder, CO, USA). BCRF was measured on both leaf surfaces, i.e. from the adaxial (upper) and the abaxial (lower) leaf side. Three measurements were made with the contact probe on each side of the leaf, each measurement being the average of 25 spectroradiometer scans. The BCRF of leaf sample was expressed as reflectance relative to the BCRF of the white reference panel.

Assessment of leaf structural and anatomical traits

Quantitative anatomical traits of leaf internal structure were measured on leaf samples excised from the middle of one half from the same leaf a leaf blade. Leaf segments (squares of 0.5 cm²) of leaf samples were fixed in formalin – acetic acid – alcohol (FAA) fixative (70% ethanol, 40% formaldehyde, glacial acetic acid, 90:5:5, v/v). The leaf segments were cut by hand microtome, and the leaf cross sections were stained with toluidine blue

for better contrast to visualized cell walls (O'Brien et al., 1964). Leaf cross-sections (about 50–80 µm thick) were mounted in a slide and observed by bright field microscope Olympus B×40 with magnification 40×. We acquired three images of each of five cross sections per each leaf segment by camera (EOS100D, Canon Inc., Tokyo, Japan), mounted to the microscope. Example of the microphotographs is provided in Figure 1. These microphotographs were used for measuring leaf anatomical traits in ImageJ image analysis software (<https://imagej.net/>, accessed on 31 March 2021). Simple measurement of a distance of two manually marked points was used for all anatomical parameters. The following leaf internal structure traits were derived: LT, PP and SP thickness, and upper (UE, i.e. adaxial) and lower (LE, i.e. abaxial) epidermis thickness.

Biochemical assessment of leaf pigments

After measuring the BCRF, one leaf disc (area = 68 mm²) was taken for photosynthetic pigment analysis and another leaf disc was taken for anthocyanin assessment.

Photosynthetic pigments (chlorophyll a+b (Chl), and total carotenoids (Car)) were assessed spectrophotometrically from dimethylformamide extracts (Porra et al., 1989). Pigment content was calculated according to (Wellburn, 1994) and pigments were related to leaf area. Anthocyanins (Anth) were extracted in acidified methanol according to (Mancinelli et al., 1975) and converted to molar concentration using the Beer-Lambert equation with the universal molar extinction coefficient $\epsilon = 30,000 \text{ L} \cdot \text{mol}^{-1} \cdot \text{cm}^{-1}$ (Merzlyak et al., 2008) and related to leaf area.

Descriptive statistics

Differences in the leaf traits among species are shown in the Table 1. For each species, descriptive statistics

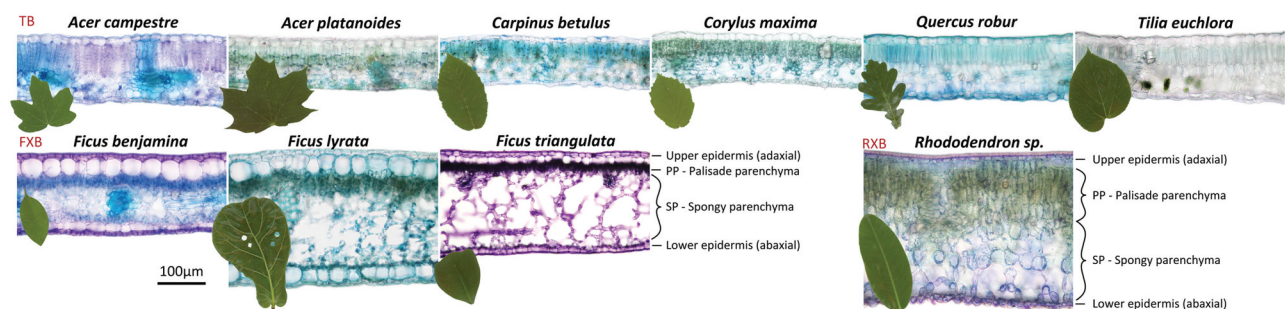


Figure 1. Anatomical micrographs of cross sections of studied tree and shrub species with macroscopic leaf photos placed in the left of the cross section. Group 1: TB – temperate broadleaved species in the first row (*Acer campestre* L., *Acer platanoides* L., *Carpinus betulus* L., *Corylus maxima* L., *Quercus robur* L. and *Tilia euchlora* C. Koch). Group two: FXB – *Ficus* xeromorphic broadleaved species (*Ficus benjamina* L., *Ficus lyrata* Warb. And *Ficus triangularis* L.). Group tree: RXB – *Rhododendron* xeromorphic broadleaved species. The line segment in lower left corner corresponds to 100 µm in all cross sections presented; the macro photos of green leaves are presented without its actual scale. Light microscopy, bright field, stained with toluidine blue.

Table 1. Summary of descriptive statistics for all biophysical traits per species.

	<i>Acer campestre</i> (N = 6)	<i>Acer platanoides</i> (N = 7)	<i>Carpinus betulus</i> (N = 6)	<i>Corylus maxima</i> (N = 6)	<i>Ficus benjamina</i> (N = 7)	<i>Ficus lyrata</i> (N = 3)	<i>Ficus triangularata</i> (N = 6)	<i>Quercus robur</i> (N = 7)	<i>Rhododendron sp.</i> (N = 6)	<i>Tilia euchlora</i> (N = 6)	Overall (N = 60)
Chl ($\mu\text{g}\cdot\text{cm}^{-2}$)											
Mean (SD)	20.5 (13)	19.2 (17.6)	21.4 (14.7)	21.9 (11.1)	41.1 (18.8)	59.5 (8.64)	62.2 (8.93)	30.3 (19.9)	40 (28.2)	28.1 (21.4)	32.9 (21.7)
Median [Min, Max]	20.4 [0.48, 34.9]	15.5 [0.88, 43.5]	22.7 [1.94, 40.9]	25.3 [1.38, 31.3]	37.0 [15.5, 67.3]	56.0 [53.2, 69.4]	61.0 [53.2, 74.3]	19.1 [7.31, 58.1]	45.6 [1.30, 78.4]	24.7 [0.24, 55.3]	30.1 [0.24, 78.4]
Car ($\mu\text{g}\cdot\text{cm}^{-2}$)											
Mean (SD)	2.99 (1.44)	3.92 (1.14)	4.11 (0.99)	3.36 (1.2)	4.91 (2.76)	7.59 (1.01)	7.02 (1.14)	4.68 (1.68)	6.72 (3.21)	3.13 (2.11)	4.69 (2.28)
Median [Min, Max]	3.11 [0.96, 4.5]	4.09 [2.12, 5.56]	4.01 [2.64, 5.51]	3.41 [1.51, 5.01]	4.84 [1.34, 8.75]	7.49 [6.63, 8.64]	7.14 [5.29, 8.72]	4.51 [2.20, 7.03]	6.57 [2.72, 11.4]	2.29 [1.16, 5.92]	4.29 [0.96, 11.4]
Car/Chl											
Mean (SD)	0.45 (0.76)	1.28 (2)	0.49 (0.7)	0.3 (0.39)	0.12 (0.02)	0.12 (0.01)	0.11 (0.01)	0.22 (0.18)	0.64 (1.19)	1.18 (2.66)	0.51 (1.19)
Median [Min, Max]	0.15 [0.12, 2]	0.14 [0.11, 5.4]	0.15 [0.13, 1.88]	0.14 [0.13, 1.09]	0.13 [0.09, 0.13]	0.12 [0.12, 0.13]	0.115 [0.1, 0.12]	0.14 [0.12, 0.62]	0.17 [0.13, 3.07]	0.11 [0.08, 6.61]	0.13 [0.08, 6.61]
Anth (nmol$\cdot\text{cm}^{-2}$)											
Mean (SD)	7.62 (4.42)	22.5 (15.2)	8.26 (8)	46.6 (53.1)	13.2 (8.49)	19.6 (12.7)	7.08 (3.32)	9.16 (7.52)	32.5 (13.9)	9.48 (6.27)	17.6 (21.9)
Median [Min, Max]	7.75 [0.47, 11.5]	21.1 [7.21, 51.8]	5.82 [0.86, 20.6]	23.8 [19.9, 154]	12.7 [5.06, 23]	20.0 [6.72, 32.1]	6.92 [2.53, 11.9]	8.47 [0.71, 21.4]	34.0 [11.2, 48.2]	7.01 [3.81, 18.4]	11.4 [0.47, 154]
LMA ($\mu\text{g}\cdot\text{cm}^{-2}$)											
Mean (SD)	4.87 (2.49)	3.81 (1.34)	4.42 (0.9)	3.40 (1.1)	5.62 (1.5)	9.98 (0.92)	4.77 (1.05)	4.19 (1.23)	9.88 (3.59)	3.08 (0.84)	5.13 (2.68)
Median [Min, Max]	3.9 [2.72, 8.7]	3.71 [1.96, 6.07]	4.18 [3.40, 6.04]	3.24 [2.28, 4.73]	5.64 [3.21, 8.28]	10.4 [8.93, 10.7]	5.36 [3.35, 5.52]	4.42 [2.46, 5.54]	9.39 [4.20, 14.9]	3.41 [2, 3.85]	4.46 [1.96, 14.9]
EWT ($\mu\text{g}\cdot\text{cm}^{-2}$)											
Mean (SD)	7.81 (1)	6.70 (1.1)	7.17 (1.91)	6.61 (1.35)	12.4 (0.8)	19.2 (1.88)	17.9 (1.22)	7.45 (1.55)	18.6 (2.8)	8.25 (1.03)	10.7 (5.02)
Median [Min, Max]	8.1 [6.40, 8.86]	6.32 [5.43, 8.33]	6.81 [5.14, 9.99]	6.41 [5.17, 8.97]	12.2 [11.4, 13.6]	19.4 [17.3, 21]	18.0 [15.7, 19.2]	7.08 [5.43, 9.65]	18.9 [15.2, 23]	8.26 [6.5, 9.44]	8.64 [5.14, 23]
LD ($\mu\text{g}\cdot\text{cm}^{-3}$)											
Mean (SD)	362 (154)	363 (75.4)	407 (45.1)	324 (73.9)	305 (72.6)	348 (31.9)	115 (22.5)	368 (89.8)	264 (36.4)	234 (50.2)	309 (108)
Median [Min, Max]	308 [224, 644]	384 [236, 431]	428 [348, 451]	318 [235, 423]	307 [183, 429]	336 [324, 384]	124 [81.7, 135]	393 [230, 492]	280 [208, 298]	243 [157, 288]	302 [81.7, 644]
LT (μm)											
Mean (SD)	131 (22.9)	103 (18.8)	108 (14.4)	103 (11.4)	183 (11.1)	287 (18.7)	411 (24.3)	113 (11.2)	375 (151)	131 (17.8)	187 (122)
Median [Min, Max]	133 [102, 167]	98.7 [83.1, 141]	104 [96.5, 134]	104 [90.7, 117]	183 [171, 200]	277 [275, 309]	410 [371, 446]	108 [102, 132]	326 [202, 648]	132 [101, 157]	133 [83.1, 648]
PP (μm)											
Mean (SD)	45.5 (12.8)	34.7 (13.1)	32.7 (4.96)	28.4 (5.96)	30.1 (6.02)	37.7 (3.12)	38.5 (9.53)	31.3 (5.48)	107 (60.3)	32.4 (5.07)	41.6 (29.5)
Median [Min, Max]	46.6 [31.4, 65]	33.2 [23.6, 61.6]	32.3 [25.2, 40.3]	28.5 [21.4, 36.8]	29.6 [21.1, 38.4]	37.0 [35.0, 41.2]	38.0 [24.8, 54.2]	29.9 [25.4, 39.4]	89.7 [36.3, 209]	33.5 [23.7, 37.1]	35.0 [21.1, 209]
SP (μm)											
Mean (SD)	52.6 (8.92)	36.4 (4.3)	47.2 (9.04)	46.6 (6.85)	80.0 (4.44)	159 (19.5)	292 (23.5)	51.6 (4.74)	211 (69.5)	59.4 (12)	98.4 (86.4)
Median [Min, Max]	52.6 [39.9, 65.6]	36.3 [31.8, 44.5]	44.7 [39.1, 62.7]	49.1 [33.8, 53.5]	80.4 [71.6, 85.7]	149 [146, 181]	298 [258, 319]	50.1 [47.5, 60.1]	197 [122, 336]	56.2 [47.2, 82.3]	55.9 [31.8, 336]
UE (μm)											
Mean (SD)	17.5 (2.87)	17.2 (1.37)	13.7 (2.05)	14.1 (2.12)	48.3 (4.7)	51.1 (0.9)	50.5 (5.8)	15.0 (1.39)	33.8 (16.9)	18.9 (3.04)	26.8 (16)
Median [Min, Max]	16.9 [15, 22.8]	16.6 [15.5, 19.3]	13.8 [11.1, 16.2]	14.4 [10.4, 16.7]	49.7 [42.4, 54.3]	50.8 [50.3, 52.1]	49.8 [42.9, 58]	14.7 [13.2, 17.2]	31.4 [17.3, 64.4]	19.3 [14.3, 23]	17.9 [10.4, 64.4]
LE (μm)											
Mean (SD)	11.1 (1.33)	11.1 (1.3)	10.8 (1.15)	10.2 (1.89)	20.6 (2.18)	32.0 (0.62)	22.1 (1.89)	11.7 (1.15)	16.9 (6.85)	14.4 (1.33)	15.2 (6.2)
Median [Min, Max]	11.2 [9.53, 12.9]	11.3 [9.14, 12.9]	11.1 [8.69, 11.9]	10.7 [8.02, 12.3]	20.7 [17.7, 24]	32.1 [31.4, 32.6]	21.8 [20.0, 25.6]	11.5 [10.6, 13.8]	14.2 [12.2, 30.6]	15.0 [11.9, 15.4]	12.3 [8.02, 32.6]
PP/LT											
Mean (SD)	0.34 (0.04)	0.33 (0.05)	0.3 (0.02)	0.28 (0.03)	0.16 (0.02)	0.13 (0.02)	0.09 (0.02)	0.28 (0.02)	0.27 (0.06)	0.25 (0.02)	0.25 (0.09)
Median [Min, Max]	0.35 [0.28, 0.39]	0.34 [0.27, 0.44]	0.31 [0.26, 0.32]	0.29 [0.23, 0.32]	0.16 [0.12, 0.19]	0.13 [0.11, 0.15]	0.09 [0.06, 0.13]	0.27 [0.24, 0.31]	0.28 [0.18, 0.34]	0.24 [0.22, 0.27]	0.27 [0.06, 0.44]
SP/LT											
Mean (SD)	0.4 (0.02)	0.36 (0.02)	0.43 (0.02)	0.45 (0.05)	0.44 (0.02)	0.55 (0.03)	0.71 (0.03)	0.46 (0.01)	0.58 (0.04)	0.46 (0.05)	0.48 (0.1)
Median [Min, Max]	0.4 [0.38, 0.43]	0.36 [0.32, 0.39]	0.43 [0.41, 0.47]	0.46 [0.37, 0.51]	0.44 [0.41, 0.46]	0.54 [0.53, 0.59]	0.72 [0.66, 0.74]	0.45 [0.45, 0.48]	0.6 [0.52, 0.62]	0.46 [0.4, 0.53]	0.45 [0.32, 0.74]
PP/SP											
Mean (SD)	0.86 (0.13)	0.93 (0.23)	0.7 (0.06)	0.62 (0.14)	0.37 (0.07)	0.24 (0.05)	0.13 (0.04)	0.6 (0.06)	0.48 (0.14)	0.56 (0.1)	0.57 (0.26)
Median [Min, Max]	0.87 [0.66, 0.99]	0.94 [0.7, 1.38]	0.69 [0.64, 0.78]	0.62 [0.46, 0.78]	0.37 [0.26, 0.45]	0.25 [0.19, 0.28]	0.13 [0.08, 0.2]	0.6 [0.5, 0.68]	0.46 [0.3, 0.65]	0.53 [0.43, 0.68]	0.59 [0.08, 1.38]

are reported, including mean, standard deviation (SD) and median, minimum (Min), maximum (Max) of all biophysical traits gained analytically.

Partial least squares regression – PLSR

PLSR was fitted with the kernel algorithm and root mean square error of prediction (RMSEP) was gained in cross-validation with leave-one-out method. Each PLSR was trained with using of whole spectral range (350–2500 nm) and biophysical traits or their ratios, with 60 repeats (Table 2). PLSR were constructed using pls package (Liland et al., 2022) in R software (R Core Team, 2021).

The models were evaluated based on the standard measures (Heise et al., 2005), such as the lowest number of components used for model fitting (a measure of model robustness), the lowest RMSEP, and the value of explained variance (transformed to coefficient of determination (R^2)) (Table 2) (Mevik & Wehrens, 2015)). The RMSEP value was related to the range of the leaf biophysical trait used for PLSR fitting using percentage (RMSEP %).

Results

Differences in leaf anatomical structure among tree species

The leaf internal structure for all studied species is shown in Figure 1 using leaf cross sections. The micro-photographs are representative of fully developed leaves of the sampled species with no signs of senescence (collection date 16th September). The studied tree species leaves were organised into 3 groups, which showed similar leaf structural traits as presented in Figure 1.

Group one (Figure 1, TB, from left to right) is comprised of temperate broadleaved leaves, which had similar leaf thickness and similar PP/SP ratio,

with sparse spongy mesophyll cells having large inter-cellular space adjacent to the lower epidermis.

Group two (Figure 1, FXB) included *Ficus* xeromorphic broadleaved leaves, which exhibited pronounced epidermal surfaces with thick cuticle, upper epidermis having two distinctive layers and PP forming only thin though very dense layer comparing to very sparse and thick SP. Altogether the PP/SP ratio had the smallest values for FXB group.

Group three (Figure 1, RXB) includes *Rhododendron* xeromorphic broadleaved species with a pronounced, cuticle, also two-layered in the UE, though with more dense photosynthetic tissue – mesophyll, where PP was multi-layered and dense, and the PP/SP ratio was significantly higher comparing to FXB leaves.

Species specific variance within the leaf biophysical properties

Based on the descriptive statistics for all traits presented in Table 1, there was remarkable variability in several leaf traits, especially in pigment contents (Chl, Car, carotenoids to chlorophyll a+b ratio (Car/Chl), Anth) in TB and RXB species. The observed range of the leaf traits is likely affected due to averaging trait values for three time points within the growing season (spring, late summer, fall). Leaf mass per area and EWT depend on accumulation structural compounds (cellulose, lignin) during to growing season as well, so the variability is mainly in TB and RXB species. FXB species grown indoor do not show such big variability in pigment contents, leaf mass per area and EWT. The anatomical traits (leaf mass density, LT, PP, SP, UE thickness, LE thickness), show low variability in all three studied species groups. Leaf structure was probably fully developed in TB and RXB species at the time of the first sampling and did not change but remained stable during the season. Seasonal variation is not present in FXB species due to indoor environment although leaves of different ages were sampled.

Table 2. Statistical parameters of partial least squares regression (PLSR) for studied leaf traits. The models were derived using the BCRF from the upper (adaxial) and lower (abaxial) leaf sides using the measurements from all functional groups and species together.

	PLSR model based on BCRF from ADAXIAL = UPPER leaf side						PLSR model based on BCRF from ABAXIAL = LOWER leaf side					
	comps	RMSE	Min	Max	RMSEP%	R^2	comps	RMSE	Min	Max	RMSEP%	R^2
Chl ($\mu\text{g}\cdot\text{cm}^{-2}$)	4	5.84	0.24	78.40	7.47	0.95	6	8.56	0.24	78.40	10.95	0.90
Car ($\mu\text{g}\cdot\text{cm}^{-2}$)	7	0.96	0.96	11.40	9.23	0.89	9	1.13	0.96	11.40	10.81	0.89
Car/Chl	7	0.02	0.08	6.61	0.32	0.64	8	0.02	0.08	6.61	0.30	0.72
Anth ($\text{nmol}\cdot\text{cm}^{-2}$)	4	9.36	0.47	154.00	6.10	0.40	6	9.05	0.47	154.00	5.90	0.53
LMA ($\mu\text{g}\cdot\text{cm}^{-2}$)	7	1.35	1.96	14.92	10.40	0.83	10	1.21	1.96	14.92	9.33	0.91
EWT ($\mu\text{g}\cdot\text{cm}^{-2}$)	7	1.65	5.14	22.96	9.27	0.93	7	1.79	5.14	22.96	10.06	0.93
LT μm	7	60.45	83.10	648.00	10.70	0.86	9	53.75	83.10	648.00	9.51	0.90
PP/LT	7	0.04	0.06	0.44	11.76	0.84	9	0.04	0.06	0.44	11.17	0.89
SP/LT	8	0.06	0.32	0.74	12.94	0.84	10	0.04	0.32	0.74	8.59	0.94
PP/SP	8	0.15	0.08	1.43	11.30	0.84	10	0.15	0.08	1.43	10.97	0.87
LD ($\mu\text{g}\cdot\text{cm}^{-3}$)	6	70.55	81.72	644.03	12.55	0.68	6	65.28	81.72	644.03	11.61	0.74
UE (μm)	5	8.60	10.40	64.40	15.92	0.81	5	8.63	10.40	64.40	15.99	0.80
LE (μm)	5	3.96	8.02	32.60	16.09	0.68	5	3.82	8.02	32.60	15.52	0.73

Variation in the thickness of different tissues (LT, PP thickness, SP thickness, UE thickness, LE thickness) is apparent in Figure 1, similarly as are the differences of the internal structure asymmetry among the species groups. TB species have comparable LT, PP thickness, SP thickness, UE thickness, LE thickness, and ratio of the PP/SP thickness. However, TB species visually differ from the RXB and FXB species in the internal anatomy (Table 1). Even though, RXB species has similar ratio of the PP/LT, SP/LT and PP/SP as TB species, its LT is rather closer to FXB species and two times thicker than in TB species.

In FXB species is visible multi-layered UE, with a single layer of big globular epidermal cells, suppressed PP thickness and pronounced low-density SP with large volume of intercellular spaces. The ratio of PP/SP in FXB species is remarkably lower than in the TB and RXB species. LT of the FXB species is higher than TB species and *F. lyrata* has even LT comparable with *Rhododendron* species.

PLSR models performance

We produced PLSR models, where the leaf optical properties (BCRF) from 350–2500 nm of all species together served as independent variables X and measured leaf biophysical and anatomical traits were then dependent variables Y. The model performance was evaluated according to the R^2 of the trained PLSR and RMSEP of its cross-validation. The parameters of all trained models using reflectance measured from upper and lower leaf side are presented in Table 2. Relationship between the measured traits to the PLSR models is visible in Table 1, where diversity in the species ensure a large range in the measured traits, especially in the structural traits.

The traits with highest portion of explained variability (R^2) and lowest error in percentage (RMSEP %) were as follows: Chl ($R^2 = 0.95$); Car ($R^2 = 0.89$); Car/Chl ($R^2 = 0.72$); Anth ($R^2 = 0.53$); LMA ($R^2 = 0.91$); EWT ($R^2 = 0.93$); LT ($R^2 = 0.90$); PP/LT ($R^2 = 0.89$); SP/LT ($R^2 = 0.94$); LD ($R^2 = 0.74$); UE ($R^2 = 0.81$); LE ($R^2 = 0.73$).

For the Chl, and UE, the PLSR model performed better for BCRF obtained from the adaxial side of the leaf. Surprisingly, the estimation for Anth content performed better using BCRF measured on the abaxial side of the leaf. For the anatomical traits LT, PP/LT, SP/LT, and PP/SP ratio and leaf mass density, the PLSR models performed better if based on abaxial BCRF. For the Car and EWT, the model explained same proportion of the variability regardless orientation of BCRF measurement. However, the normalized RMSEP for carotenoids and EWT PLSR models was lower for adaxial BCRF.

Discussion

PLSR models

Methods for estimation and quantification of individual leaf traits from reflectance at various hierarchical scales (e.g. leaf and canopy) are rapidly advancing. Recently a broad spectrum of machine learning algorithms were tested and applied for leaf functional traits retrieval (Fu et al., 2019; Verrelst et al., 2019). PLSR is one of the linear nonparametric regression methods that deal with the co-linearity in hyperspectral data. PLSRs are often used for biophysical leaf traits retrieval such as nitrogen, chlorophyll, carotenoid, water, structural and defence components or mineral nutrients content (Chavana-Bryant et al., 2019; Chen et al., 2022; Lhotáková et al., 2021; Martin & Aber, 1997; Serbin et al., 2014; Singh et al., 2015; Wang et al., 2022).

The PLSR exhibits superior robustness against noise in spectral data compared to alternative methods (e.g.: stepwise multiple linear regression), and it is particularly well-suited for small datasets (as ours in the present paper) and can handle a higher number of spectral wavebands than available samples (Atzberger et al., 2010). Still, it is important to deal with outliers in leaf trait measurements, as they have the potential to compromise estimation accuracy. Additionally, the training dataset must encompass a sufficient amount of variance in the data to ensure validity, particularly at the extremes of leaf trait distributions (Burnett et al., 2021). Burnett et al. (2021) address the challenges associated with the development of single-purpose models and emphasized the importance of investigating the generalizability of PLSR method. For developing accurate predictive PLSR models, the datasets for leaf traits training and validation should be based on the same species, with comparable physiological status, ontogenetic stage and phenological phase. It is necessary to note that despite the mentioned advantages of PLSR, the nonlinear nonparametric modelling methods such as decision trees and artificial neural networks may outperform linear regression models for leaf traits retrieval (Verrelst et al., 2019).

Even though leaf structural properties determine leaf photosynthetic functioning (Terashima et al., 2011), studies focused on their retrieval from leaf spectra are rare. Several studies address the leaf anatomical traits correlation with vegetation indices or specific (usually NIR) wavelengths (Bandaru et al., 2010; Neuwirthová et al., 2021; Slaton et al., 2001). The very first attempt to model PP thickness from leaf spectra by PLSR has been done on holm oak (*Quercus ilex*) (Ourcival et al., 1999) with excellent model performance ($R^2 = 0.97$ and three model components), which was even better if the second derivative spectra transformation was used.

For retrieval of the leaf anatomical traits the PLSR approach was also used in our previous study for detection of leaf surface structure based on leaf specular reflection (Neuwirthová, Lhotáková et al., 2021). The study was conducted on several herbaceous species of *Hieracium* genus, and even though the variance in leaf traits was rather small, the PLSR model training on LT, PP and SP thickness was promising (R^2 ranging between 0.63 and 0.75 with three to four model components). In the present study, the models showed very good performance in terms of higher R^2 and lower RMSEP% than in (Neuwirthová, Lhotáková et al., 2021). However, the models in the present study were always trained with higher number of components (7–10) than in our previous study.

In recent years, innovative methods based on machine learning principles, such as neural networks, or methods based on support vector regression and Gaussian process regression, have become increasingly popular. These are made available to the remote sensing community by tools such as ARTMO (Caicedo et al., 2014; Verrelst et al., 2011, 2019). Potentially, some increase in the predictive abilities of the predictive models could be achieved using these approaches. However, the relative differences in the predictive abilities for individual traits and the differences in the ability to predict these traits from the adaxial or abaxial side could be expected to be maintained.

Environmental drivers of the leaf internal structure and their implications to leaf optical properties

Leaf internal structure determines the biophysical environment within the leaf. Larger volume of intercellular space in thicker leaves causes higher reflectance and lower transmittance (Woolley, 1971) particularly in the NIR (Slaton et al., 2001). Thicker leaves with greater surface area of chloroplasts exposed to the intercellular airspaces usually have better leaf CO_2 transfer conductance and thus higher photosynthetic rates (Evans et al., 1994; Hanba et al., 2001). In present study we used the hand-sections, which are easy and quick to prepare, without time-consuming pre-processing typical for paraffin or plastic sections. However, the detailed anatomical traits, such as internal leaf surface of chloroplast surface exposed to intercellular space could not be derived from this data due to limitations of section thickness and light microscopy. For more detailed information on 3D leaf structure, advanced microscopy and tomography techniques are required in combination with machine learning algorithms to evaluate large number of samples (Thérourx-Rancourt et al., 2020). Even the simple leaf anatomical traits that we measured such as LT, PP, and SP thickness (Table 1) may bring an

insight into the vegetation functioning. For the PLSR modelling we used the ratios of measured leaf and tissue thicknesses: PP/LT, SP/LT, PP/SP (Table 2) for their correlation to ecophysiology plant functions. As shown by (Neuwirthová et al., 2021), both the SP/LT and PP/SP are closely related to water use efficiency and gross primary production at the regional scale. In the same study (Neuwirthová et al., 2021) observed that LT, ratios PP/SP, PP/LT, SP/LT and SP thickness significantly correlated with the mean annual temperature and precipitation of the site. Leaf anatomical traits could also be related to plant climate change response. The PP/SP ratio was shown to correlate with photosynthetic heat tolerance in Asian mangrove species (Li et al., 2022). As the anatomical studies are time consuming and restrict greater sample numbers for statistical evaluation, it appears to be advantageous to predict them from leaf optical properties.

Thus, for the present study we focused on dorsiventral leaf structure, which is most common for mesomorphic terrestrial vegetation of temperate region. However, to cover more variability on studied structural parameters, we included two groups of dorsiventral xeromorphic leaves – *Ficus* spp. and *Rhododendron* sp., which differed particularly in PP/SP ratio. Both groups of xeromorphic leaves, though, exhibited great difference in structure and density of the upper and lower side of the leaf, more pronounced than for typical mesomorphic dorsiventral leaves.

In some biophysical parameters models performed better based on the BCRF from the side of the leaf that is closer to the modelled biophysical parameter. For example, photosynthetic pigments Chl were modelled better based on the adaxial (upper) BCRF same as adaxial (upper) epidermis, (see Table 2). Also model estimating abaxial (lower) epidermis was better from abaxial (lower) BCRF. Surprisingly, the estimation for Car/Chl ratio and Anth content performed better from BCRF based on the abaxial side of the leaf. However, for the anatomical traits (LMA, LD, LT, ratios of PP/LT, SP/LT, PP/SP), the PLSR models performed better if based on lower leaf side BCRF as evident in Table 2. This result is probably due to strong differences in the PP and SP thicknesses, (what is reflecting also in the LT variance). Another aspect is different effect of PP and SP on light scattering within the leaf interior. More isotropic SP cells with high proportion of intercellular spaces and high internal leaf surface comparing to PP cells, produce light scattering at the cell wall-air space interface and leads to an increase in light absorption and reflection and a decrease in transmittance, particularly in the near infrared (NIR) region (McClendon & Fukshansky, 1990a, 1990b; Parry et al., 2014). Moreover, mesomorphic leaves with less dense mesophyll are known to have a lower internal-external surface ratio and lower chlorophyll concentration than the xeromorphic leaves as it was reported already in 1930's by (Turrell, 1939). The proportion of intercellular

spaces is remarkably lower towards the upper leaf side compared to the average values of the dorsiventral leaf, while the relative chlorophyll content across the leaf profile stays rather constant (Borsuk & Brodersen, 2019).

The derived models of leaf anatomy (Table 2) yielded optimal results using abaxial reflectance, potentially due to leaf protective adaptations, such as thicker epidermal walls and presence of waxes and other protective compounds on the leaf adaxial surface, which serve to limit the absorption of the incoming radiation. As a result, the adaxial reflectance signal is augmented or depends much less on the internal leaf anatomy, than on the leaf position and distribution angles in relation to the incident light.

Implications of dorsiventral leaf optical properties for radiative transfer modelling (RTM) and remote sensing (RS)

Detailed anatomical traits such as the proportion of PP/SP are often neglected in the leaf level optical studies, although internal structure governs leaf physiological function (He et al., 2018; Liu et al., 2019). Neglecting the two-sided optical properties at the leaf level could result in a 20% underestimation of top-of-canopy reflectance (Lukeš et al., 2020).

Incorporating internal leaf structure, especially the adaxial-abaxial internal tissue asymmetry determined by species specificity, environmental factors, and leaf phenological development during the season into radiative transfer models (RTMs), (QSPEC (Ma et al., 2007), dorsiventral leaf model (DLM), (Stuckens et al., 2009), ISPECT (Shi et al., 2023), simplified version of the FASPECT (Jiang et al., 2021)) brings more information about the biological reality observed in-situ into remote sensing studies (Lukeš et al., 2020). At the leaf level also the 3D RTM models are emerging, which take into account very detailed leaf structure such as dimensions and wall thickness of various cell types constructing leaf mockup with combination of Monte Carlo ray tracing (Kallel, 2018, 2020). Typically, most current radiative transfer models, except for those with explicit representations of 3D structure (e.g. the voxel-based DART model), do not account for the dorsiventral asymmetry of optical properties observed in nature and assume identical optical properties of the top and bottom of the leaf. Moreover, these models are most often coupled with the PROSPECT model (Jacquemoud & Baret, 1990; Wu et al., 2021). The latter is very popular because of its simplicity and low number of input parameters (the internal structure of the leaf is represented by a single parameter, the so-called N number, which describes the number of layers, i.e. a proxy of the leaf optical thickness), but by its nature it does not allow to simulate separately

the adaxial and abaxial optical properties of the leaf. For operational deployment, the most commonly used canopy radiative transfer models (e.g. SAIL (Verhoef, 1984)) would need to incorporate the ability to parameterize the dorsiventral asymmetry of optical properties and use simplified models of sheet-level optical properties with this capability (e.g. the DLM model).

Conclusion

Our goal of this study was to establish if there are differences in the performance of PLSR models for selected leaf-level traits from BCRF values measured from the abaxial and adaxial sides of leaves. The results demonstrated that differences in dorsiventral leaf reflectance (here determined by BCRF combining measurements from both sides of the leaf), driven by internal structure, have a direct effect on trait prediction models using PLSR. This finding complies well with the prior reports that PLSR models for deriving leaf-level traits of total chlorophyll content exhibit greater accuracy when using BCRF measurements collected from the adaxial side. In comparison, traits describing leaf structure (e.g. LMA, EWT, LT, PP and SP ratios) can be described better by PLSR models generated from abaxial BCRF leaf measurements.

The study supports conclusion that internal asymmetry in leaf structure affects significantly leaf optical properties and should not be neglected in radiative transfer modelling at the leaf level and when upscaling leaf properties to canopy level. Some of the important implications for future studies, include: 1) laboratory measurements of leaf optical properties for quantifying leaf-level traits can be improved by selecting trait-specific measurements of adaxial reflectance (leaf biochemistry) and abaxial reflectance (leaf structure), and 2) trait-specific measurements can improve the accuracy of the estimated leaf anatomical properties, which can help to better parameterisation of the next generation of leaf-level RTMs. Using RTMs that incorporate both biochemical and anatomical inputs, ecosystem function can be investigated and modelled with greater accuracy.

Acknowledgments

The study was funded by the Ministry of Education, Youth and Sports of the Czech Republic, scheme INTER-EXCELLENCE, project No. LTAUSA18154. The contribution of Petya Campbell was supported by NASA grants NNH17ZDA001N and 80NSSC24K0044. Lucie Červená was partly supported in the phase of writing by Charles University UNCE/HUM 018. We thank to Miroslav Barták (CUNI) for graphical technical help, Drahomíra Bartáková and Zdeňka Češpírová (CUNI) for help with leaf hand sectioning and cross section analyses.

Disclosure statement

The authors declare that the research was conducted in the absence of any commercial or financial relationships that could be construed as a potential conflict of interest.

Funding

The work was supported by the Ministry of Education Youth and Sports [INTER-EXCELLENCE, LTAUSA18154]; by the National Aeronautics and Space Administration [NNH17ZDA001N; 80NSSC24K0044]; and by Charles University [UNCE/HUM 018].

ORCID

Eva Neuwirthová  <http://orcid.org/0000-0001-5613-847X>
 Zuzana Lhotáková  <http://orcid.org/0000-0003-3060-641X>
 Lucie Červená  <http://orcid.org/0000-0001-5246-1106>
 Petr Lukeš  <http://orcid.org/0000-0002-3707-6557>
 Petya Campbell  <http://orcid.org/0000-0002-0505-4951>
 Jana Albrechtová  <http://orcid.org/0000-0001-6912-1992>

Data availability statement

The data presented in this study are available on reasonable request from the corresponding author.

References

- Atzberger, C., Guérif, M., Baret, F., & Werner, W. (2010). Comparative analysis of three chemometric techniques for the spectroradiometric assessment of canopy chlorophyll content in winter wheat. *Computers and Electronics in Agriculture*, 73(2), 165–173. <https://doi.org/10.1016/j.compag.2010.05.006>
- Bandaru, V., Hansen, D. J., Codling, E. E., Daughtry, C. S., White-Hansen, S., & Green, C. E. (2010). Quantifying arsenic-induced morphological changes in spinach leaves: Implications for remote sensing. *International Journal of Remote Sensing*, 31(15), 4163–4177. <https://doi.org/10.1080/01431161.2010.498453>
- Borsuk, A. M., & Brodersen, C. R. (2019). The spatial distribution of chlorophyll in leaves. *Plant Physiology*, 180(3), 1406–1417. <https://doi.org/10.1104/pp.19.00094>
- Borsuk, A. M., Roddy, A. B., Théroux-Rancourt, G., & Brodersen, C. R. (2022). Structural organization of the spongy mesophyll. *New Phytologist*, 234(3), 946–960. <https://doi.org/10.1111/nph.17971>
- Burnett, A. C., Anderson, J., Davidson, K. J., Ely, K. S., Lamour, J., Li, Q., Morrison, B. D., Yang, D., Rogers, A., Serbin, S. P., & Lawson, T. (2021). A best-practice guide to predicting plant traits from leaf-level hyperspectral data using partial least squares regression. *Journal of Experimental Botany*, 72(18), 6175–6189. <https://doi.org/10.1093/jxb/erab295>
- Buschmann, C., Lenk, S., & Lichtenthaler, H. K. (2012). Reflectance spectra and images of green leaves with different tissue structure and chlorophyll content. *Israel Journal of Plant Sciences*, 60(1), 49–64. <https://doi.org/10.1560/IJPS.60.1-2.49>
- Caicedo, J. P. R., Verrelst, J., Muñoz-Marí, J., Moreno, J., & Camps-Valls, G. (2014). Toward a semiautomatic machine learning retrieval of biophysical parameters. *IEEE Journal of Selected Topics in Applied Earth Observations and Remote Sensing*, 7(4), 1249–1259. <https://doi.org/10.1109/JSTARS.2014.2298752>
- Campbell, P. K. E., Huemmrich, K. F., Middleton, E. M., Ward, L. A., Julitta, T., Daughtry, C. S. T., Burkart, A., Russ, A. L., & Kustas, W. P. (2019). Diurnal and seasonal variations in chlorophyll fluorescence associated with photosynthesis at leaf and canopy scales. *Remote Sensing*, 11(5), 488. <https://doi.org/10.3390/rs11050488>
- Campbell, P. K. E., Middleton, E. M., McMurtry, J. E., Corp, L. A., & Chappelle, E. W. (2007). Assessment of vegetation stress using reflectance or fluorescence measurements. *Journal of Environmental Quality*, 36(3), 832–845. <https://doi.org/10.2134/jeq2005.0396>
- Cao, K.-F. (2000). Leaf anatomy and chlorophyll content of 12 woody species in contrasting light conditions in a Bornean heath forest. *Canadian Journal of Botany*, 78(10), 1245–1253. <https://doi.org/10.1139/b00-096>
- Chavana-Bryant, C., Malhi, Y., Anastasiou, A., Enquist, B. J., Cosio, E. G., Keenan, T. F., & Gerard, F. F. (2019). Leaf age effects on the spectral predictability of leaf traits in Amazonian canopy trees. *Science of the Total Environment*, 666, 1301–1315. <https://doi.org/10.1016/j.scitotenv.2019.01.379>
- Chávez, R. O., Clevers, J. G. P. W., Verbesselt, J., Naulin, P. I., Herold, M., & Schumann, G. J. P. (2014). Detecting leaf pulvinar movements on NDVI time series of desert trees: A New approach for water stress detection. *PLoS ONE*, 9(9), e106613. <https://doi.org/10.1371/journal.pone.0106613>
- Chen, L., Zhang, Y., Nunes, M. H., Stoddart, J., Khoury, S., Chan, A. H. Y., & Coomes, D. A. (2022). Predicting leaf traits of temperate broadleaf deciduous trees from hyperspectral reflectance: Can a general model be applied across a growing season? *Remote Sensing of Environment*, 269, 112767. <https://doi.org/10.1016/j.rse.2021.112767>
- Díaz, S., Lavorel, S., de Bello, F., Quétier, F., Grigulis, K., & Robson, T. M. (2007). Incorporating plant functional diversity effects in ecosystem service assessments. *Proceedings of the National Academy of Sciences*, 104(52), 20684–20689. <https://doi.org/10.1073/pnas.0704716104>
- Eitel, J. U. H., Gessler, P. E., Smith, A. M. S., & Robberecht, R. (2006). Suitability of existing and novel spectral indices to remotely detect water stress in Populus spp. *Forest Ecology and Management*, 229(1–3), 170–182. <https://doi.org/10.1016/j.foreco.2006.03.027>
- Evans, J. R., Caemmerer, S. V., Setchell, B. A., & Hudson, G. S. (1994). The relationship between CO₂ transfer conductance and leaf anatomy in transgenic tobacco with a reduced content of Rubisco. *Functional Plant Biology*, 21(4), 475–495.
- Fu, P., Meacham-Hensold, K., Guan, K., & Bernacchi, C. J. (2019). Hyperspectral leaf reflectance as proxy for photosynthetic capacities: An ensemble approach based on multiple machine learning algorithms. *Frontiers in Plant Science*, 10. <https://doi.org/10.3389/fpls.2019.00730>
- Gastellu-Etchegorry, J. P., Martin, E., & Gascon, F. (2004). DART: A 3D model for simulating satellite images and studying surface radiation budget. *International Journal of Remote Sensing*, 25(1), 73–96. <https://doi.org/10.1080/0143116031000115166>
- Gates, D., Keegan, H., Schleter, J., & Weidner, V. (1965). Spectral properties of plants. *Applied Optics*, 4(1), 11. <https://doi.org/10.1364/AO.4.000011>
- Hallik, L., Kuusk, A., Lang, M., & Kuusk, J. (2019). Reflectance properties of Hemiboreal mixed forest

- canopies with focus on Red edge and near infrared spectral regions. *Remote Sensing*, 11(14), 1717. <https://doi.org/10.3390/rs11141717>
- Hanba, Y. T., Miyazawa, S. I., Kogami, H., & Terashima, I. (2001). Effects of leaf age on internal CO₂ transfer conductance and photosynthesis in tree species having different types of shoot phenology. *Functional Plant Biology*, 28(11), 1075–1084.
- Hanba, Y. T., Miyazawa, S.-I., & Terashima, I. (1999). The influence of leaf thickness on the CO₂ transfer conductance and leaf stable carbon isotope ratio for some evergreen tree species in Japanese warm-temperate forests. *Functional Ecology*, 13(5), 632–639. <https://doi.org/10.1046/j.1365-2435.1999.00364.x>
- Heise, H. M., Damm, U., Lampen, P., Davies, A. N., & McIntyre, P. S. (2005). Spectral variable selection for partial least squares calibration applied to authentication and quantification of extra virgin olive oils using fourier transform raman Spectroscopy. *Applied Spectroscopy*, 59(10), 1286–1294. <https://doi.org/10.1366/000370205774430927>
- He, N., Liu, C., Tian, M., Li, M., Yang, H., Yu, G., Guo, D., Smith, M. D., Yu, Q., Hou, J., & Niu, S. (2018). Variation in leaf anatomical traits from tropical to cold-temperate forests and linkage to ecosystem functions. *Functional Ecology*, 32(1), 10–19. <https://doi.org/10.1111/1365-2435.12934>
- Jacquemoud, S., & Baret, F. (1990). Prospect: A model of leaf optical properties spectra. *Remote Sensing of Environment*, 34(2), 75–91. [https://doi.org/10.1016/0034-4257\(90\)90100-Z](https://doi.org/10.1016/0034-4257(90)90100-Z)
- Jiang, J., Comar, A., Weiss, M., & Baret, F. (2021). FASPECT: A model of leaf optical properties accounting for the differences between upper and lower faces. *Remote Sensing of Environment*, 253, 112205. <https://doi.org/10.1016/j.rse.2020.112205>
- Kallel, A. (2018). Leaf polarized BRDF simulation based on monte carlo 3-D vector RT modeling. *Journal of Quantitative Spectroscopy and Radiative Transfer*, 221, 202–224. <https://doi.org/10.1016/j.jqsrt.2018.09.033>
- Kallel, A. (2020). FluLCVRT: Reflectance and fluorescence of leaf and canopy modeling based on Monte Carlo vector radiative transfer simulation. *Journal of Quantitative Spectroscopy and Radiative Transfer*, 253, 107183. <https://doi.org/10.1016/j.jqsrt.2020.107183>
- Kenzo, T., Ichie, T., Yoneda, R., Kitahashi, Y., Watanabe, Y., Ninomiya, I., & Koike, T. (2004). Interspecific variation of photosynthesis and leaf characteristics in canopy trees of five species of dipterocarpaceae in a tropical rain forest. *Tree Physiology*, 24(10), 1187–1192. <https://doi.org/10.1093/treephys/24.10.1187>
- Knapp, A. K., & Carter, G. A. (1998). Variability in leaf optical properties among 26 species from a broad range of habitats. *American Journal of Botany*, 85(7), 940–946. <https://doi.org/10.2307/2446360>
- Lhotáková, Z., Kopačková-Strnadová, V., Oulehle, F., Homolová, L., Neuwirthová, E., Švik, M., Janoutová, R., & Albrechtová, J. (2021). Foliage biophysical trait prediction from laboratory spectra in Norway spruce is more affected by needle age than by site soil conditions. *Remote Sensing*, 13(3), 391. <https://doi.org/10.3390/rs13030391>
- Liland, K. H., Mevik, B.-H., & Wehrens, R. (2022). Pls: Partial Least Squares and Principal component regression. R package version 2.8-1. <https://CRAN.R-project.org/package=pls>
- Liu, C., Li, Y., Xu, L., Chen, Z., & He, N. (2019). Variation in leaf morphological, stomatal, and anatomical traits and their relationships in temperate and subtropical forests. *Scientific Reports*, 9(1), 5803. <https://doi.org/10.1038/s41598-019-42335-2>
- Li, X., Wen, Y., Chen, X., Qie, Y., Cao, K.-F., Wee, A. K. S., & Adams, W. (2022). Correlations between photosynthetic heat tolerance and leaf anatomy and climatic niche in Asian mangrove trees. *Plant Biology*, 24(6), 960–966. <https://doi.org/10.1111/plb.13460>
- Lukeš, P., Neuwirthová, E., Lhotáková, Z., Janoutová, R., & Albrechtová, J. (2020). Upscaling seasonal phenological course of leaf dorsiventral reflectance in radiative transfer model. *Remote Sensing of Environment*, 246, 111862. <https://doi.org/10.1016/j.rse.2020.111862>
- Ma, K., Baret, F., Barroy, P., & Bousquet, L. (2007). A leaf optical properties model accounting for differences between the two faces. International Society for Photogrammetry and Remote Sensing.
- Mancinelli, A. L., Yang, C.-P. H., Lindquist, P., Anderson, O. R., & Rabino, I. (1975). Photocontrol of anthocyanin synthesis. *Plant Physiology*, 55(2), 251–257. <https://doi.org/10.1104/pp.55.2.251>
- Martin, M. E., & Aber, J. D. (1997). High spectral resolution Remote Sensing of forest canopy lignin, nitrogen, and ecosystem processes. *Ecological Applications*, 7(2), 431–443. [https://doi.org/10.1890/1051-0761\(1997\)007\[0431:HSRRSO\]2.0.CO;2](https://doi.org/10.1890/1051-0761(1997)007[0431:HSRRSO]2.0.CO;2)
- McClendon, J. H. (1962). The relationship between the thickness of deciduous leaves and their maximum photosynthetic rate. *American Journal of Botany*, 49(4), 320–322. <https://doi.org/10.1002/j.1537-2197.1962.tb14944.x>
- McClendon, J. H., & Fukshansky, L. (1990a). On the interpretation of absorption spectra of leaves—I. Introduction and the correction of leaf spectra for surface reflection. *Photochemistry and Photobiology*, 51(2), 203–210. <https://doi.org/10.1111/j.1751-1097.1990.tb01704.x>
- McClendon, J. H., & Fukshansky, L. (1990b). On the interpretation of absorption spectra of leaves—II. The non-absorbed ray of the sieve effect and the mean optical pathlength in the remainder of the leaf. *Photochemistry and Photobiology*, 51(2), 211–216. <https://doi.org/10.1111/j.1751-1097.1990.tb01705.x>
- Merzlyak, M. N., Chivkunova, O. B., Solovchenko, A. E., & Naqvi, K. R. (2008). Light absorption by anthocyanins in juvenile, stressed, and senescing leaves. *Journal of Experimental Botany*, 59(14), 3903–3911. <https://doi.org/10.1093/jxb/ern230>
- Mevik, B. H., & Wehrens, R. (2015). Introduction to the pls Package. *Help section of the “Pls” package of R studio software*, 1–23.
- Middleton, E. M., Huemmrich, K. F., Zhang, Q., Campbell, P. K., & Landis, D. R. (2018). Photosynthetic efficiency and vegetation stress. In *Biophysical and Biochemical Characterization and Plant Species Studies* (pp. 133–179). CRC Press.
- Neuwirthová, E., Kuusk, A., Lhotáková, Z., Kuusk, J., Albrechtová, J., & Hallik, L. (2021). Leaf age matters in Remote Sensing: Taking ground truth for spectroscopic studies in hemiboreal deciduous trees with continuous leaf formation. *Remote Sensing*, 13(7), 1353. <https://doi.org/10.3390/rs13071353>
- Neuwirthová, E., Lhotáková, Z., Lukeš, P., & Albrechtová, J. (2021). Leaf surface reflectance does not affect biophysical traits modelling from VIS-NIR spectra in plants with sparsely distributed trichomes. *Remote Sensing*, 13(20), 4144. <https://doi.org/10.3390/rs13204144>
- Niinemets, Ü. (2001). Global-scale climatic controls of leaf dry mass per area, density, and thickness in trees and

- shrubs. *Ecology*, 82(2), 453–469. [https://doi.org/10.1890/0012-9658\(2001\)082\[0453:GSCCOL\]2.0.CO;2](https://doi.org/10.1890/0012-9658(2001)082[0453:GSCCOL]2.0.CO;2)
- Niklas, K. J. (1991). The elastic moduli and mechanics of populus tremuloides (salicaceae) petioles in bending and torsion. *American Journal of Botany*, 78(7), 989–996. <https://doi.org/10.1002/j.1537-2197.1991.tb14503.x>
- O'Brien, T. P., Feder, N., & McCully, M. E. (1964). Polychromatic staining of plant cell walls by toluidine blue O. *Protoplasma*, 59(2), 368–373. <https://doi.org/10.1007/BF01248568>
- Orcival, J. M., Joffre, R., & Rambal, S. (1999). Exploring the relationships between reflectance and anatomical and biochemical properties in quercus ilex leaves. *New Phytologist*, 143(2), 351–364. <https://doi.org/10.1046/j.1469-8137.1999.00456.x>
- Parry, C., Blonquist, J. M., & Bugbee, B. (2014). In situ measurement of leaf chlorophyll concentration: Analysis of the optical/absolute relationship: The optical/absolute chlorophyll relationship. *Plant, Cell & Environment*, 37(11), 2508–2520. <https://doi.org/10.1111/pce.12324>
- Pastenes, C. (2004). Leaf movements and photoinhibition in relation to water stress in field-grown beans. *Journal of Experimental Botany*, 56(411), 425–433. <https://doi.org/10.1093/jxb/eri061>
- Porra, R., Thompson, W., & Kriedemann, P. (1989). Determination of accurate extinction coefficients and simultaneous-equations for assaying chlorophyll-a and chlorophyll-B extracted with 4 different solvents—verification of the concentration. *Biochimica Et Biophysica Acta*, 975(3), 384–394. [https://doi.org/10.1016/S0005-2728\(89\)80347-0](https://doi.org/10.1016/S0005-2728(89)80347-0)
- R Core Team. (2021). *R: A language and environment for statistical computing*. R Foundation for Statistical Computing.
- Roden, J. S. (2003). Modeling the light interception and carbon gain of individual fluttering aspen (Populus tremuloides Michx) leaves. *Trees*, 17(2), 117–126. <https://doi.org/10.1007/s00468-002-0213-3>
- Serbin, S. P., Singh, A., Mcneil, B. E., Kingdon, C. C., & Townsend, P. A. (2014). Spectroscopic determination of leaf morphological and biochemical traits for northern temperate and boreal tree species. *Ecological Applications*, 24(7), 19.
- Shi, H., Jiang, J., Jacquemoud, S., Xiao, Z., & Ma, M. (2023). Estimating leaf mass per area with leaf radiative transfer model. *Remote Sensing of Environment*, 286, 113444. <https://doi.org/10.1016/j.rse.2022.113444>
- Shull, C. A. (1929). A spectrophotometric study of reflection of light from leaf surfaces. *Botanical Gazette*, 87(5), 583–607. <https://doi.org/10.1086/333965>
- Singh, A., Serbin, S. P., McNeil, B. E., Kingdon, C. C., & Townsend, P. A. (2015). Imaging spectroscopy algorithms for mapping canopy foliar chemical and morphological traits and their uncertainties. *Ecological Applications*, 25(8), 2180–2197. <https://doi.org/10.1890/14-2098.1>
- Slaton, M. R., Hunt, E. R., & Smith, W. K. (2001). Estimating near-infrared leaf reflectance from leaf structural characteristics. *American Journal of Botany*, 88(2), 278–284. <https://doi.org/10.2307/2657019>
- Slaton, M. R., & Smith, W. K. (2002). Mesophyll architecture and cell exposure to intercellular air space in Alpine, desert, and forest species. *International Journal of Plant Sciences*, 163(6), 937–948. <https://doi.org/10.1086/342517>
- Stuckens, J., Verstraeten, W. W., Delalieux, S., Swennen, R., & Coppin, P. (2009). A dorsiventral leaf radiative transfer model: Development, validation and improved model inversion techniques. *Remote Sensing of Environment*, 113(12), 2560–2573. <https://doi.org/10.1016/j.rse.2009.07.014>
- Terashima, I., Hanba, Y. T., Tholen, D., & Niinemets, Ü. (2011). Leaf functional anatomy in relation to photosynthesis. *Plant Physiology*, 155(1), 108–116. <https://doi.org/10.1104/pp.110.165472>
- Thérour-Rancourt, G., Jenkins, M. R., Brodersen, C. R., McElrone, A., Forrester, E. J., & Earles, J. M. (2020). Digitally deconstructing leaves in 3D using X-ray micro-computed tomography and machine learning. *Applications in Plant Sciences*, 8(7), e11380. <https://doi.org/10.1002/aps3.11380>
- Turrell, F. M. (1939). The relation between chlorophyll concentration and the internal surface of mesomorphic and xeromorphic leaves grown under artificial light. *Proceedings of the Iowa Academy of Science*, 46(1), 107–117.
- Verhoef, W. (1984). Light scattering by leaf layers with application to canopy reflectance modeling: The SAIL model. *Remote Sensing of Environment*, 16(2), 125–141. <https://doi.org/10.1016/0034-42578490057-9>
- Verrelst, J., Malenovsky, Z., Van der Tol, C., Camps-Valls, G., Gastellu-Etchegorry, J.-P., Lewis, P., North, P., & Moreno, J. (2019). Quantifying vegetation biophysical variables from Imaging Spectroscopy data: A review on retrieval methods. *Surveys in Geophysics*, 40(3), 589–629. <https://doi.org/10.1007/s10712-018-9478-y>
- Verrelst, J., Rivera, J. P., Alonso, L., & Moreno, J. (2011). ARTMO: An automated radiative transfer models operator toolbox for automated retrieval of biophysical parameters through model inversion. 9.
- Villar, R., Ruiz-Robledo, J., Ubert, J. L., & Poorter, H. (2013). Exploring variation in leaf mass per area (LMA) from leaf to cell: An anatomical analysis of 26 woody species. *American Journal of Botany*, 100(10), 1969–1980. <https://doi.org/10.3732/ajb.1200562>
- Vogelmann, T. C. (1993). Plant Tissue Optics. *Annual Review of Plant Biology*, 44(1), 231–251. <https://doi.org/10.1146/annurev.pp.44.060193.001311>
- Wang, Z., Townsend, P. A., & Kruger, E. L. (2022). Leaf spectroscopy reveals divergent inter- and intra-species foliar trait covariation and trait–environment relationships across NEON domains. *New Phytologist*, 235(3), 923–938. <https://doi.org/10.1111/nph.18204>
- Wellburn, A. R. (1994). The spectral determination of chlorophylls a and b, as well as total carotenoids, using various solvents with spectrophotometers of different resolution. *Journal of Plant Physiology*, 144(3), 307–313. [https://doi.org/10.1016/S0176-1617\(11\)81192-2](https://doi.org/10.1016/S0176-1617(11)81192-2)
- Woolley, J. T. (1971). Reflectance and transmittance of light by leaves. *Plant Physiology*, 47(5), 656–662. <https://doi.org/10.1104/pp.47.5.656>
- Wu, S., Zeng, Y., Hao, D., Liu, Q., Li, J., Chen, X., Asrar, G. R., Yin, G., Wen, J., Yang, B., Zhu, P., & Chen, M. (2021). Quantifying leaf optical properties with spectral invariants theory. *Remote Sensing of Environment*, 253, 112131. <https://doi.org/10.1016/j.rse.2020.112131>
- Yang, S.-J., Sun, M., Zhang, Y.-J., Cochard, H., & Cao, K.-F. (2014). Strong leaf morphological, anatomical, and physiological responses of a subtropical woody bamboo (sinarundinaria nitida) to contrasting light environments. *Plant Ecology*, 215(1), 97–109. <https://doi.org/10.1007/s11258-013-0281-z>
- Zhang, X., Jin, G., & Liu, Z. (2019). Contribution of leaf anatomical traits to leaf mass per area among canopy layers for five coexisting broadleaf species across shade tolerances at a regional scale. *Forest Ecology and Management*, 452, 117569. <https://doi.org/10.1016/j.foreco.2019.117569>